J Therm Anal Calorim (2009) 97:99–103
DOI 10.1007/s10973-009-0074-8

Thermogravimetric and UV–vis spectroscopic studies of chromium redox reactions in rutile pigments

F. T. G. Vieira · Soraia C. Souza · A. L. M. Oliveira · S. J. G. Lima · E. Longo · C. A. Paskocimas · L. E. B. Soledade · A. G. Souza · Iêda M. G. Santos

Received: 25 September 2008 / Accepted: 13 February 2009 / Published online: 24 June 2009

Abstract In this study undoped and Cr, Sb or Mo doped TiO_2 were synthesized by polymeric precursor method and characterized by X-ray diffraction, UV–VIS spectroscopy, infrared spectroscopy and thermogravimetry (TG). The TG curves showed a continuous mass loss assigned to the hydroxyl elimination and Cr^{6+} reduction. Doped TiO_2 samples showed a higher mass loss assigned to water and gas elimination at lower temperatures. In these doped materials a decrease in the anatase–rutile phase transition temperature was observed. After calcination at 1,000 °C, rutile was obtained as a single phase material without the presence of Cr^{6+}.

Keywords Pechini · Thermal analysis · TiO_2 · Redox reactions

F. T. G. Vieira · S. C. Souza · A. L. M. Oliveira · L. E. B. Soledade · A. G. Souza · I. M. G. Santos (✉)
Laboratório de Combustíveis e Materiais, Departamento de Química, Universidade Federal da Paraíba, Campus I, João Pessoa, PB, Brazil
e-mail: ieda@quimica.ufpb.br

S. J. G. Lima
LSR, Departamento de Engenharia Mecânica/CT, Universidade Federal da Paraíba, Campus I, João Pessoa, PB, Brazil

E. Longo
CMDMC-LIEC, Instituto de Química, UNESP, Araraquara, SP, Brazil

C. A. Paskocimas
Departamento de Engenharia de Materiais, Universidade Federal do Rio Grande do Norte, Natal, RN, Brazil

Introduction

Several methods have been reported for the successful determination and quantification of Cr^{6+}, a toxic pollutant and attributed some carcinogenic activity. Some of them rely on spectroscopic techniques, while others depend on mass-sensitive devices and electrochemical detection [1].

The oxidation state and localization of the chromium ions in the host matrix have been investigated by means of X-ray absorption near-edge (XANES), extended X-ray absorption fine structure (EXAFS), optical absorption and electron spin resonance (ESR) spectroscopies. The local environment of the chromium cations in the host matrix, as well as their oxidation state also determine the optical properties of the pigments [2]. Depending on the host lattice and synthesis conditions a variety of oxidation states were observed for chromium, antimony and molybdenum [3].

As a consequence of doping the physical properties of the TiO_2 solid solutions are modified including the phase transition temperature of the anatase–rutile phase [4]. Previous studies [5] showed that the oxidation of Cr^{3+} to Cr^{6+} progressively decreases with temperature and stops at 1,200 °C. At the same time the reddish lilac color ascribed to the Cr^{6+} species also vanished. It is important to remark that after calcinations at 1,300 °C, at which temperature the violet color was developed, no traces of Cr^{6+} were noticed.

In this work undoped and Cr, Sb or Mo doped TiO_2 samples were synthesized using the polymeric precursor method [6–9]. The redox reactions were followed by using thermogravimetry and UV–VIS spectroscopy. The samples were also characterized by X-ray diffraction (XRD) and infrared spectroscopy. Chromium was used as chromophore and antimony or molybdenum were used as counter ions. UV–VIS peaks, ascribed to diverse oxidation states of chromium, antimony and molybdenum were noticed.

Experimental

Undoped and Cr, Sb or Mo doped TiO_2 samples were synthesized using the Pechini polymeric precursor method. Initially titanium citrate was prepared using citric acid (Cargill) and titanium isopropoxide (Hulls) according to [7–9]. After the synthesis of the titanium citrate adequate amounts of chromium (III), molybdenum (VI) or antimony (III) precursors were added to the solution in order to obtain the samples with the following stoichiometries: TiO_2, $Ti_{0.94}Cr_{0.06}O_2$, $Ti_{0.89}Cr_{0.06}Sb_{0.05}O_2$ and $Ti_{0.90}Cr_{0.06}Mo_{0.04}O_2$. A 3:1 citric acid:metal molar ratio was used. Chromium (III) acetate hydroxide (Alfa Aesar), antimony (III) oxide (Merck) were used as chromium and antimony precursors. For molybdenum doping, molybdenum citrate synthesized from molybdic acid—Dinâmica, was utilized.

The final solution was then mixed with ethylene glycol and heated to promote the esterification reactions in the solution. The chelated metal ions remained homogenously distributed throughout the polymeric network. Then, the samples were calcined at 300 °C for 1 h leading to the formation of the powder precursors. These precursors were de-agglomerated in a mortar, passing through a 100 mesh sieve and milled in an attritor mill, for 4 h in alcohol. These powder precursors were submitted to a second heat treatment at about 300–350 °C for 12 h. A third heat treatment was carried out at and at 600–1,000 °C for 2 h in an oxygen atmosphere. More details of the experimental part can be found in [6–9].

The powder precursors were examined by thermogravimetry as well the samples after the second heat treatments. The TG curves were recorder using a SDT 2960, TA Instruments analyzer. An O_2 atmosphere was used with a flow rate of 110 mL min^{-1}. The samples were heated at 10 °C min^{-1} heating rates up to 1,000 °C. About 10 mg of sample were weighted in alumina crucibles.

The X-ray diffraction patterns have been obtained in a Siemens D-5000 diffractometer using a monochromatic CuKα target. The crystalline phases (anatase and rutile) were evaluated in a semi-quantitative way according to Spurr Myers Equation (1) [10].

$$\%\text{rutile} = \frac{1}{1 + 0.8\frac{I_{\text{anatase}}}{I_{\text{rutilo}}}} * 100 \quad (1)$$

where: I_{anatase} and I_{rutile} are the intensities of the (101) and (110) peaks of anatase and rutile phases, respectively.

Infrared spectroscopy was carried out in a BOMEM MB 102-series equipment, using KBr pellets. The sample was vigorously milled in a mortar yielding a very fine powder. For the preparation of the infrared pellets about 100–150 mg of the heat treated material was used blended with a tiny amount of KBr, previously dried in an oven at 100 °C. Both materials are then vigorously milled again, blended and later pressed, in order to obtain a thin and transparent pellet.

The samples heat treated at 600–1,000 °C for 2 h in an oxygen atmosphere were compacted in order to become denser. Later their UV–VIS spectra were obtained using an UV-2550 Shimadzu spectrophotometer, in the 190–900 nm range.

Results and discussion

The thermogravimetric curves of undoped TiO_2 precursor (Fig. 1) presented two mass loss steps. The first one was assigned to the release of physically adsorbed water and gases adsorbed on the powder precursor surface [7, 8]. The highest mass loss of the first step was related to the undoped sample, possibly due to highly hygroscopic character of TiO_2. Previous studies indicate that the second step is related to the combustion of the organic material leading to the formation of CO_2 and H_2O [7, 8]. In the present work, this step was assigned to the elimination of hydroxyls and residual organic material. Only a small mass loss was observed and no exothermic peak was present in the DTA curve, indicating that a high amount of carbon was eliminated during calcination in oxygen atmosphere.

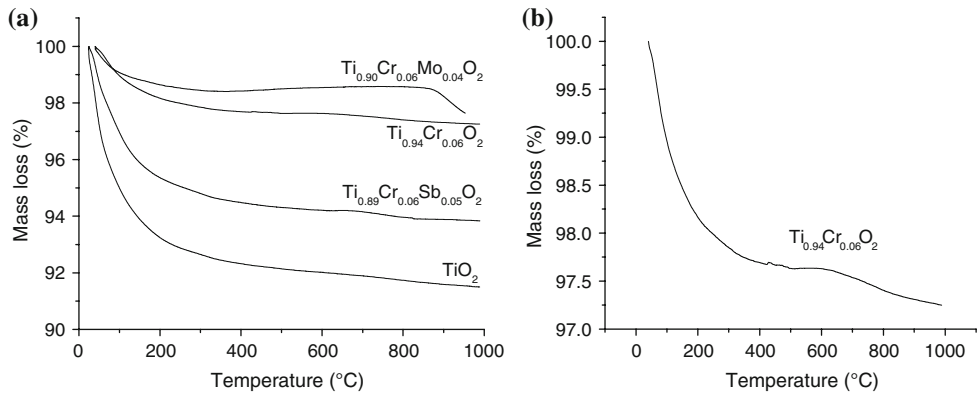

Fig. 1 Thermogravimetric curves of the doped and undoped TiO_2 precursors (**a**) and $Ti_{0.94}Cr_{0.06}O_2$ (**b**)

Table 1 Temperature and mass loss values determined by TG

Sample	1st step		2nd step		3rd step	
	Temperature range (°C)	Mass variation (%)	Temperature range (°C)	Mass variation (%)	Temperature range (°C)	Mass variation (%)
TiO_2	25–300	−7.6	350–980	−1.0	–	–
TiO_2: Cr	40–300	−2.2	350–500	−0.2	580–980	−0.4
TiO_2: Cr, Sb	28–350	−5.4	350–603	−0.4	673–850	−0.3
TiO_2: Cr, Mo	40–350	−1.6	350–643	+0.2	816–954	−1.0

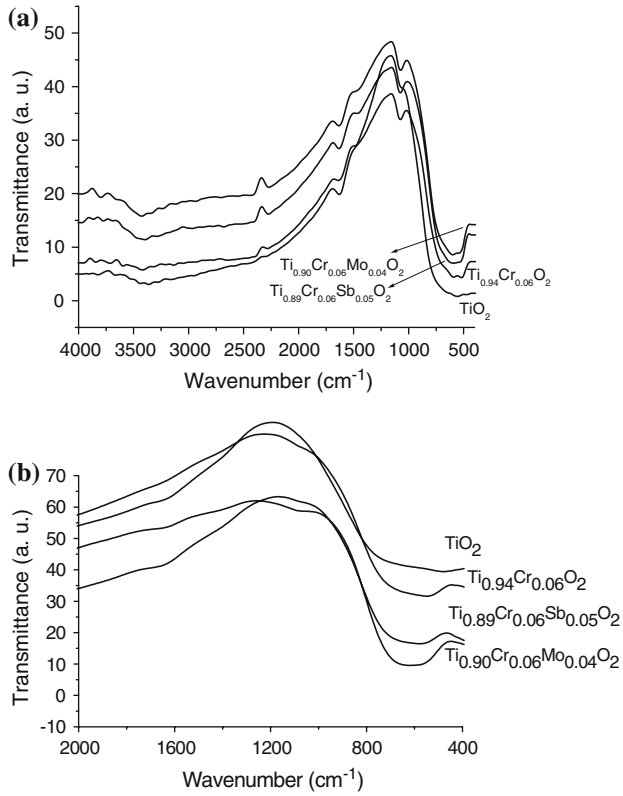

Fig. 2 Infrared spectra of TiO_2: Cr, Sb or Mo pigments, heat treated at ~330 °C for 12 h (**a**) and 1,000 °C for 2 h (**b**)

When chromium was added to TiO_2, a smaller mass loss was observed. Another mass loss step occurred above 580 °C. With the antimony addition the profile was similar to the chromium doped samples. For molybdenum a different behavior was observed with a small mass gain in the second step probably due to an oxidation process and a higher mass loss in the third step (Table 1).

In order to explain the possible evolved products upon TG runs they were characterized by infrared spectroscopy (Fig. 2).

The infrared spectra after carbon elimination (Fig. 2a) showed a band at 1,630 cm^{-1}, assigned to the presence of water [11] and a band around 1,100 cm^{-1} indicating the presence of hydroxyls [12], which may be placed on the powder surface. The amount of hydroxyls was higher in the doped samples than in undoped TiO_2. Very small bands were observed between 1,430 and 1,480 cm^{-1}, indicating that only small amounts of carbonate were formed [12]. No bands assigned to esters were observed. Water and hydroxyls were eliminated with the temperature increase as indicated by the infrared spectra after calcination at 1,000 °C (Fig. 2b). These results indicated that the continuous mass loss observed in the TG curves was due to the elimination of H_2O and OH groups, confirming that the organic material was eliminated during calcination in oxygen atmosphere.

The fundamental vibrations of TiO_2 crystals appeared in IR spectra as very intense broad bands, which were ascribed to the stretching vibrations of Ti–O bonds (550–653 cm^{-1}) and Ti–O–Ti bonds (436–495 cm^{-1}). The absorption in the 700–1,000 cm^{-1} spectral range can be assigned to surface vibrations [13]. In the present work (Fig. 2a, b) two vibration bands assigned to metal-oxygen vibrations were observed: a broad one between 500 and 750 cm^{-1} and another one around 400 cm^{-1} in agreement with [12, 14]. These bands were already present after calcination at 300 °C indicating that some short-range order was already present.

In relation to the TiO_2 structure, according to literature data the anatase–rutile phase transition is strongly affected by the presence of two- and/or trivalent dopant ions used as chromophores. When these dopants are added to the material, oxygen vacancies are formed, leading to a higher diffusion in the TiO_2 lattice, which is the main mechanism leading to phase transition. When elements with oxidation state higher than (IV) are added as counter ions the phase transition reaction is inhibited due to the charge balance in the lattice [15, 16].

In the present work the simultaneous addition of chromophore and counter ions favours the anatase–rutile phase transition (Fig. 3) in comparison to undoped and chromium-doped titania. For antimony addition, almost 90% of rutile was already obtained at 600 °C.

Chromium addition during the synthesis led to the formation of oxygen vacancies as already showed in [15, 16]. Moreover the elimination of hydroxyls during heating

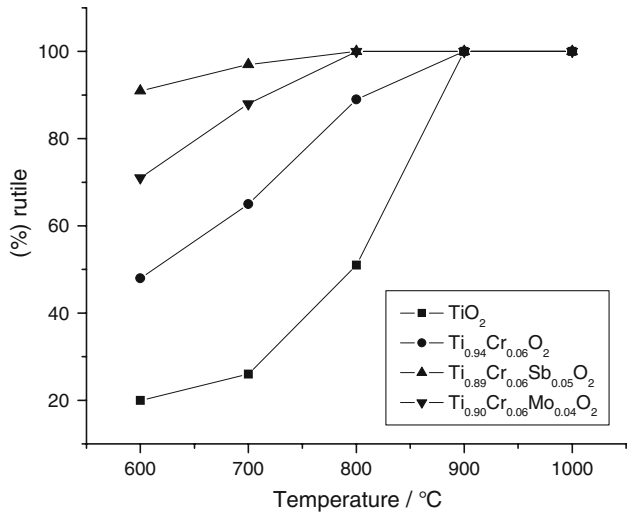

Fig. 3 Semi-quantitative analysis concerning on the amount of rutile phase in the powders

(Figs. 1, 2) can also lead to the formation of oxygen vacancies as their elimination occurs with the formation of water according to Eq. 2. As a consequence, the anatase–rutile phase transition was favored.

$$2\mathrm{Ti}-\mathrm{OH}\overset{\text{heating}}{\longrightarrow}\mathrm{Ti}-\mathrm{V}_{\mathrm{o}}^{\circ\circ}+\mathrm{Ti}-\mathrm{O}+\mathrm{H_2O}+2\mathrm{e}' \qquad (2)$$

In relation to antimony it was added to TiO_2 as Sb^{3+}, increasing the amount of oxygen vacancies and consequently, the anatase–rutile phase transition. This result may be due to the oscillation in the oxidation state of the Sb ion. During the calcinations the presence of Sb^{5+} was indicated in [17].

For molybdenum addition its reduction occurred during calcination as indicated by UV–VIS results, which showed the presence of Mo^{5+}. Its oxidation to Mo^{6+} probably occurred at higher temperatures leading to small mass gain between 350 and 643 °C can be seen in the TG curves. Above 800 °C a remarkable mass loss occurred that may due to MoO_3 sublimation.

The UV–VIS spectra were analyzed (Fig. 4) in order to evaluate the oxidation state of the cations. Chromium may be present as Cr^{3+}, Cr^{5+} and Cr^{6+}. For Cr^{3+}, bands are expected at about 15,600 cm^{-1} and 23,300 cm^{-1} due to ($^4A_2 \rightarrow {}^4T_2$) and ($^4A_2 \rightarrow {}^4T_1$) transitions [18]. A weak forbidden band at 13,500 cm^{-1} was also observed by Dondi et al. [16] for TiO_2 with rutile structure. For Cr^{5+}, transitions at 21,700 cm^{-1} occur while charge transfer transitions are present for Cr^{6+} between 27,000 and 28,000 cm^{-1} [1, 18–20]. In relation to molybdenum, Dondi et al. observed that its addition increases the absorbance all along the spectrum, presumably including Mo^{5+} absorbance bands at 13,000–14,000 cm^{-1} and 19,000–23,000 cm^{-1}. For antimony, different oxidation states may be present attributed to a change in the oxidation state, as Sb^{3+} is oxidized to Sb^{5+}. For this cation, only charge transfer transitions are observed above 20,000 cm^{-1}.

In this work, for $Ti_{0.94}Cr_{0.06}O_2$ (Fig. 4a) absorption bands were observed for Cr^{6+}, Cr^{5+} and Cr^{3+}. With the

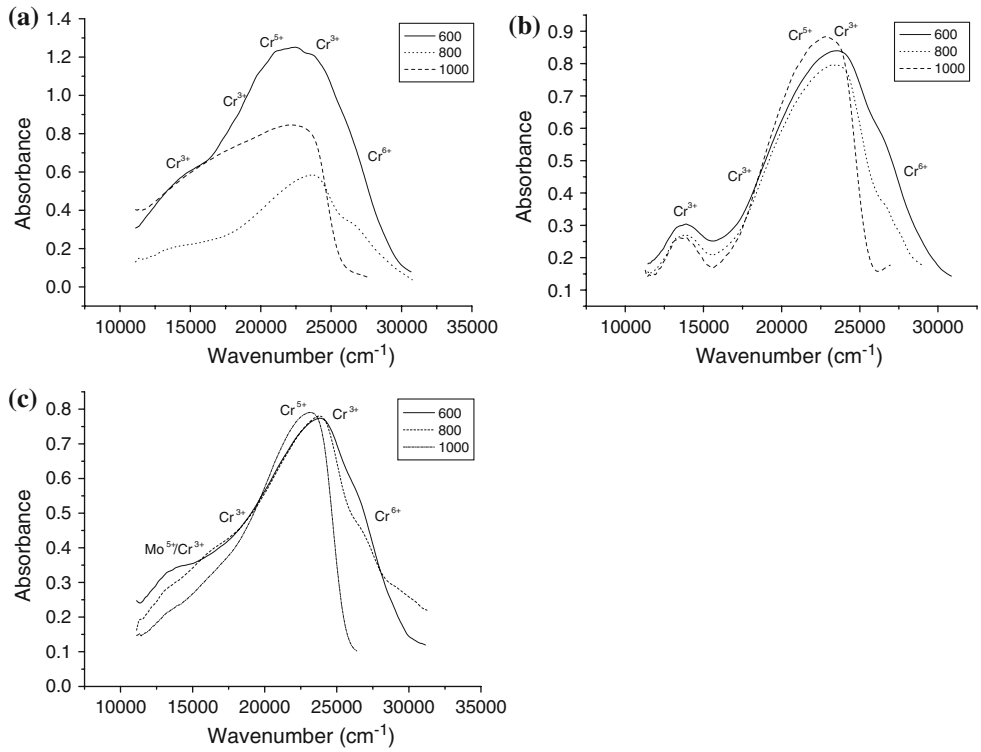

Fig. 4 UV–VIS spectra of $Ti_{0.94}Cr_{0.06}O_2$ (**a**), $Ti_{0.89}Cr_{0.06}Sb_{0.05}O_2$ (**b**) and $Ti_{0.90}Cr_{0.06}Mo_{0.04}O_2$ (**c**) after calcination at different temperatures

increase of temperature the intensity of Cr^{6+} absorption band decreased continuously and the profile of the absorption bands changed. For antimony doped samples the difference was the $^4A_{2g} \rightarrow {}^4T_{2g}$ transition of Cr^{3+} that was not observed and a higher definition of the Cr^{3+} forbidden band occurred. For molybdenum one band at about 13,300 cm^{-1} is superposed to Cr^{3+} being assigned to Mo^{5+}. The intensity of this last band decreased when the temperature increases to 1,000 °C indicating that mass loss above 800 °C may be really assigned to the molybdenum oxide sublimation. For samples containing the counter ions the profile of the absorption band did not change meaningfully with temperature increase. This was probably related to the structural stability of these samples as rutile was already the main phase after calcination at 600 °C. In all samples the amount of Cr^{6+} decreased with temperature increase, so that Cr^{6+} band at 27,000–28,000 disappeared after calcination at 1,000 °C.

The Cr^{6+} reduction may be related to the elimination of hydroxyls, which leads to the formation of free electrons in the structure. Cr^{6+} may be reduced to Cr^{5+} by a single electron and to Cr^{3+} by a three electron reduction. For molybdenum (Fig. 4c), UV–vis spectra indicated that its reduction occurred, with single electron. Thus, the small mass gain observed in the TG curve may be due to Mo^{5+} oxidation. In relation to the antimony, as already pointed out, Sb^{3+} oxidation occurs leading to the formation of Sb^{5+}. This reaction may also favor the Cr^{6+} reduction.

Conclusion

Pure and doped TiO_2 was successfully obtained by the polymeric precursor method with addition of chromium and antimony or molybdenum as counter ions. The decomposition of the powder precursor was evaluated by thermogravimetry with the aid of infrared spectroscopy and UV–VIS spectroscopy. The continuous mass loss above 300 °C was assigned to hydroxyl elimination and Cr^{6+} reduction as no exothermic peak was observed in the DTA curves and bands assigned to carbon compounds were not present in the IR spectra. Cr^{6+} reduction was favored instead of the oxidation of Sb^{3+} and Mo^{5+}. The anatase–rutile phase transition was favored for Cr doped TiO_2 and moreover by the counter ion addition. As a consequence of this higher stability a smaller difference in the profile of the UV–VIS spectra was observed leading to a higher stability of the pigment color.

Acknowledgements The authors acknowledge the financial support of CNPq/MCT, PROINFRA/FINEP.

References

1. Carrington NA, Thomas GH, Rodman DL, Beach DB, Xue ZL. Optical determination of Cr(VI) using regenerable, functionalized sol-gel monoliths. Anal Chim Acta. 2007;581:232–40.
2. Navarrete EL, Caballero A, Orera VM, Lázaro FJ, Ocaña M. Oxidation state and localization of chromium ions in Cr-doped cassiterite and Cr-doped malayaite. Acta Mater. 2003;51:2371–81.
3. Galindo R, Llusar M, Tena MA, Monrós G, Badenes JA. New pink ceramic pigment based on chromium (IV)-doped lutetium gallium garnet. J Eur Ceram Soc. 2007;27:199–205.
4. Tena MA, Llusar M, Badenes JA, Calbo J, Mónros G. Structural and electrical conductivity studies on (M,V)-TiO_2 (M = Al, Cr, Fe) rutile solid solutions at high temperature. J Mater Sci Mater Electron. 2004;15:265–70.
5. Navarrete EL, Elipe ARG, Ocaña M. Non-conventional synthesis of Cr-doped SnO_2 pigments. Ceram Int. 2003;29:385–92.
6. Souza SC, Santos IMG, Silva MRS, Cássia-Santos MR, Soledade LEB, Souza AG, et al. Influence of pH on iron doped Zn_2TiO_4 pigments. J Therm Anal Calorim. 2005;79:451–4.
7. Silva MRS, Soledade LEB, Lima SJG, Longo E, Souza AG, Santos IMG. Influence of processing conditions on the thermal decomposition of $SrTiO_3$, precursors. J Therm Anal Calorim. 2007;87: 731–5.
8. Melo DS, Santos MRC, Santos IMG, Soledade LEB, Bernardi MIB, Longo E, et al. Thermal and structural investigation of SnO_2/Sb_2O_3 obtained by the polymeric precursor method. J Therm Anal Calorim. 2007;87:697–701.
9. Souza SC, Souza MAF, Lima SJG, Santos MRC, Fernandes V J Jr, Soledade LEB, et al. The effects of Co, Ni and Mn on the thermal processing of Zn_2TiO_4 pigments. J Therm Anal Calorim. 2005;79: 455–9.
10. Spurr RA, Myres H. Quantitative analysis of anatase-rutile mixtures with an x-ray diffractometer. Anal Chem. 1957;29:760–2.
11. Bezrodna T, Puchkovska G, Shymanovska V, Baran J, Ratajczak H. IR-analysis of H-bonded H_2O on the pure TiO_2 surface. J Mol Struct. 2004;700:175–81.
12. Nakamoto K. Infrared and Raman spectra of inorganic and coordination compounds. New York: John Wiley e Sons; 1986.
13. Suresh C, Biju V, Mukundan P, Warrier KGK. Anatase to rutile transformation in sol-gel titania by modification of precursor. Polyhedron. 1998;17:3131–5.
14. Udawatte CP, Kakihana M, Yoshimura M. Low temperature synthesis of pure $SrSnO_3$ and the $(Ba_xSr_{1-x})SnO_3$ solid solution by the polymerized complex method. Solid State Ion. 2000;128: 217–26.
15. Matteucci F, Cruciane G, Dondi M, Raimondo M. The role of counterions (Mo, Nb, Sb, W) in Cr-, Mn-, Ni- and V-doped rutile ceramic pigments—Part 1. Crystal structure and phase transformations. Ceram Int. 2006;32:385–92.
16. Dondi M, Cruciane G, Guarini G, Matteucci F, Raimondo F. The role of counterions (Mo, Nb, Sb, W) in Cr-, Mn-, Ni- and V-doped rutile ceramic pigments—Part 2. Colour and technological properties. Ceram Int. 2006;32:393–405.
17. Xie J, Yang P, Yuan H, Liao J, Shen B, Yin Z, et al. Influence of Sb and Y co-doping on properties of $PbWO_4$ crystal. J Cryst Growth. 2005;275:474–80.
18. Mambrim JST, Pastore HO, Davanzo CU, Vich EJS, Nakamura O, Vargas H. Synthesis and characterization of chromium silicalite. Chem Mater. 1993;5:166–73.
19. Reinen D, Rauw W, Kesper U, Atanasov M, Güdel HU, Hazenkamp M, et al. Colour, luminescence and bonding properties of tetrahedrally coordinated chromium(IV), manganese(V) and iron(VI) in various oxide ceramics. J Alloy Compd. 1997;246: 193–208.
20. Sun B, Reddy EP, Smirniotis PG. TiO_2-loaded Cr-modified molecular sieves for 4-chlorophenol photodegradation under visible light. J Catal. 2006;237:314–21.